Experimental Analysis and Numerical Modeling Using LISA-DDB Hybrid Breakup Model of Direct Injected Gasoline Spray

Sung Wook Park, Hyung Jun Kim
Graduate School of Hanyang University,
17 Haengdang-dong, Sungdong-gu, Seoul 133-791, Korea
Chang Sik Lee*
Department of Mechanical Engineering, Hanyang University,
17 Haengdang-dong, Sungdong-gu, Seoul 133-791, Korea

This paper presents the effect of injection pressure on the atomization characteristics of high-pressure injector in a direct injection gasoline engine both experimentally and numerically. The atomization characteristics such as mean droplet size, mean velocity, and velocity distribution were measured by phase Doppler particle analyzer. The spray development, spray penetration, and global spray structure were visualized using a laser sheet method. In order to investigate the atomization process in more detail, the calculations with the LISA-DDB hybrid model were performed. The results provide the effect of injection pressure on the macroscopic and microscopic behaviors such as spray development, spray penetration, mean droplet size, and mean velocity distribution. It is revealed that the accuracy of prediction is promoted by using the LISA-DDB hybrid breakup model, comparing to the original LISA model or TAB model alone. And the characteristics of the primary and secondary breakups have been investigated by numerical approach.

Key Words: Breakup Model, Gasoline Direct Injection, Sauter Mean Diameter, KIVA, Spray Characteristic

Nomenclature

a : Major semi-axis of half-droplet
C_1 : Breakup constant for DDB model
C_D : Drag coefficient
$C_{D,sphere}$: Drag coefficient of sphere
d_0 : Injector exit diameter
d_D : Droplet diameter
d_L : Ligament diameter
k : Wavelength of a disturbance on the film
K : The liquid to gas density ratio
K_L : The most unstable wavelength of ligament
L : Axial distance from nozzle tip (mm)

---
* Corresponding Author,
  E-mail : cslee@hanyang.ac.kr
  TEL : +82-2-2290-0427; **FAX** : +82-2-2281-5286
  Department of Mechanical Engineering, Hanyang University, 17 Haengdang-dong, Sungdong-gu, Seoul 133-791, Korea. (Manuscript **Received** April 30, 2002; **Revised** July 25, 2003)

L_b : Breakup length
$\dot{m}$: Mass flow rate
N : The liquid to gas dynamic viscosity ratio
Q : Ratio of gas-to-liquid density
r : Drop radius
Re : Reynolds number
t : Film thickness at the injector exit
T : Time after start of injection
u : Axial component of sheet velocity
U : Total sheet velocity
We : Weber number
y : The distance from the c.m. of the deforming half-drop to its equator
η_0 : Amplitude of initial disturbance
η_b : Critical wave amplitude
ν : Kinematics viscosity
τ : Breakup time
ω : Ggrowth rate of a disturbance
Ω : Growth of the most unstable wave

Subscripts
l : Liquid
old : Before breakup
new : After breakup

1. Introduction

Recently, the researches about internal combustion engines have been focused on the clean combustion and low exhaust emissions and improvement of fuel consumption. A direct injection type of gasoline engine has been considered as a method to solve these problems. Besides of the reduction of exhaust emission and improved fuel consumption, a gasoline direct injection (GDI) engine has many advantages such as high thermal efficiency owing to lower pumping loss and heat loss, anti-knock characteristics from lower temperature of charge air, and high acceleration response under cold temperature. In order to use GDI engine for commercial purpose, there are several problems to be solved. The generation of unburned hydrocarbon in high load regions, NOx emission during stratified charge operation, and the accumulations of deposits at the nozzle should be reduced.

Many researchers have tried to propose the methods to solve these problems experimentally. Especially, the improvement of atomization of the fuel is very important for the clean combustion of the fuel in the engine. Lee et al. (2001) studied the development of global spray and spatial velocity distribution of the injection spray of the direct injection engine by using phase Doppler particle analyzer system and particle image velocimetry (PIV) system. And Li and Gebert (1998) compared the sprays of swirl and non-swirl nozzles of GDI engine.

During the past decades, various models for droplet breakup have been proposed for the better understanding of droplet breakup process and the more accurate predictions. O'Rourke and Amsden (1987) suggested Taylor analogy breakup (TAB) model based on the analogy between an oscillation and distorting droplet and spring mass system. Ibrahim (1993) added the non-linear effect to TAB model and proposed the droplet defor-

mation and breakup (DDB) model, which shows good accordance with experimental results in the case of high-pressure diesel spray, and WAVE model that is based on stability analysis was proposed by Reitz (1987). Because spray atomization process consists of primary and secondary breakups that have different disintegration regimes, it is more reasonable to use hybrid model, which is composed of different two models. Kim et al. (1999) used WAVE model and TAB model for the primary and secondary breakups, respectively. Schmidt et al. (1999) made new breakup model by using a linear stability analysis for primary breakup and combined it with TAB model. They reported that reasonable agreements with experimental results were obtained by using this model. The hybrid breakup models have different prediction accuracy as a functions of test conditions such as injection pressure, nozzle geometry, and physical properties of test fuel. Park et al. (2001) evaluated the prediction accuracy of hybrid breakup models in terms of spray tip penetration, mean diameter distribution, and axial mean velocity distribution.

In this article, the development process of direct-injected gasoline spray is visualized by using a Nd : YAG laser and a CCD camera, and atomization characteristics according to injection pressure are investigated by phase Doppler particle analyzer (PDPA) system. In order to simulate more accurate droplet breakup process, it is attempted to unite the primary breakup process of LISA (Linearized Instability Sheet Atomization) model and DDB (Drop Deformation and Breakup) model with new breakup constant in the KIVA-3 code.

2. Experimental Apparatus and Procedures

Figure 1 shows schematic diagram of PDPA system and a spray visualization system. The PDPA system that is composed of Ar-ion laser, laser transmitter, and laser receiver was utilized to measure the local Sauter mean diameter (SMD) and axial mean velocity. The visualization system
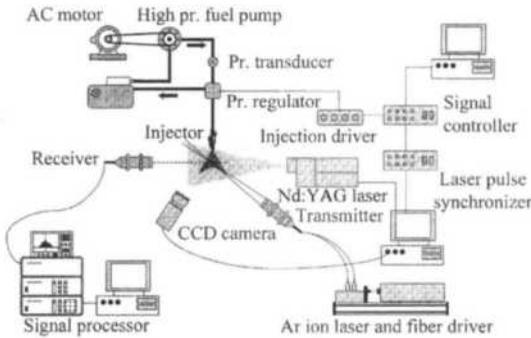
Fig. 1　Schematic diagrams of PDPA system and spray visualization system

Fig. 2　The concept of LISA-DDB hybrid model

consists of a CCD camera, optical lenses, and a Nd : YAG laser which operates at 532 nm wavelength and 50 mJ of laser power. The signals of fuel injection timing and injection duration are controlled by the computer system, signal controller, injection driver, and laser pulse synchronizer. The high-pressure injection system is composed of a fuel feed pump, a high-pressure pump, and a pressure-regulating system. The fuel is pressurized by the high-pressure pump driven by 0.75 kW AC motor, and injected through nozzle with 1 mm diameter for 1 ms of injection duration. The injected spray is analyzed by PDPA, and the sliced images are captured by spray visualization system. The experiment is conducted at the pressures of the 5 MPa and 7 MPa, in the 20 mm and 40 mm downstream from the nozzle tip.

3. Numerical Model

3.1 The construction of hybrid breakup model

Schmidt et al. (1999) proposed a new model called LISA (Linearized Instability Sheet Atomization), in which the primary breakup does not happen until droplet reaches the breakup length, and then secondary breakup is taken place by TAB (Taylor analogy breakup) model (see Fig. 2). But in the case of high-pressure injector, the spray tip penetration predicted by LISA with TAB model has lower value than the measured value despite the accuracy is increased compared to the case of TAB model alone as shown in
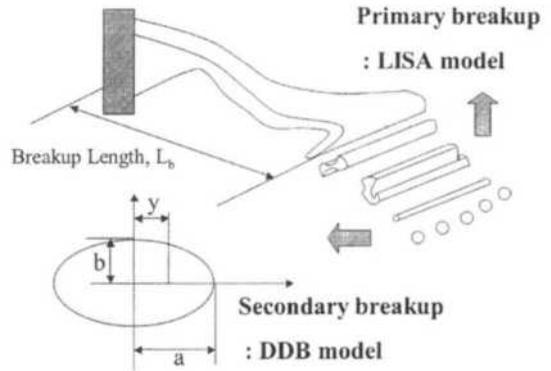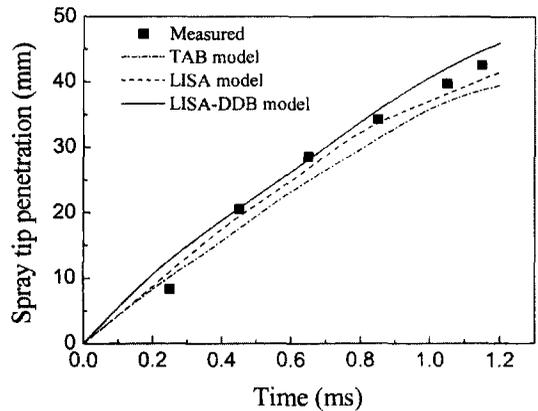

Fig. 3　Comparisons of measured and predicted spray tip penetration for different breakup models $(P_{inj} = 7$ MPa$)$

Fig. 3. In this study, to improve the prediction accuracy of breakup, TAB model has been replaced with modified DDB (Drop Deformation and Breakup) model. But original DDB model is inadequate to the hollow-cone spray because it's constant is proper several tens MPa of injection pressure. To solve this problem, the new breakup constant, C_1 is introduced to the calculation of droplet radius after breakup in this study. The initial conditions are set equal to the experimental conditions, and the initial time interval and grid are determined 20 μsec and 1 mm$\times$1 mm after the grid-dependency test.

3.2 LISA (Linearized Instability Sheet Atomization) model

For the primary breakup, LISA model is used

and it is related to the transition from internal injector flow to fully developed spray. The film thickness is governed by the mass flow rate in the film formation stage (Schmidt, 1999).

$$\dot{m} = \pi \rho u t (d_0 - t) \qquad (1)$$

This stage is governed by total sheet velocity (U) and axial component of sheet velocity (u) by injector pressure and the sheet breakup is related to maximum growth rate. So, Senecal et al. (1999) for use growth rate, ω_r is given by

$$\omega_r = 2\nu_1 k^2 + \sqrt{4\nu_1 k^4 + QU^2 k^2 - \frac{\sigma k^3}{\rho_1}} \qquad (2)$$

The maximum growth rate is found by Eq. (2) as a function of and the sheet breakup length of ligaments is given by [8]

$$L_b = U\tau = \frac{U}{\Omega} \ln\left(\frac{\eta_b}{\eta_0}\right) \qquad (3)$$

where, the value of $\ln(\eta_b/\eta_0)$ is 12 as proposed by Dombrowski and Hooper (1962). When the droplet reached to the breakup length, the drop size is determined by the following equation (Schmidt, 1999).

$$d_D^3 = \frac{3\pi d_L^2}{K_L} \qquad (4)$$

3.3 DDB (Drop Deformation and Breakup) model

After the drop size is determined by Eq. (4) at the breakup length, the droplet split into small one by DDB model. The DDB model is expressed as terms of the internal energy and the work done, and the DDB model equation is given by Ibrahim (1993)

$$K\frac{d^2 y}{dt^2} + \frac{4N}{Re}\frac{1}{y^2}\frac{dy}{dt} + \frac{27\pi^2}{16We} y[1 - 2(cy)^{-6}] = \frac{3}{8} \qquad (5)$$

The DDB model equation is solved by a fourth-order Runge-Kutta method. The initial values are $y = 4/(3\pi)$, $dy/dt = 0$ at $t = 0$. If the kinetic energy of the droplet and viscous dissipation are negligible, breakup condition is given by Ibrahim (1993)

$$\left(\frac{a}{r}\right) = \frac{We}{6\pi} \qquad (6)$$

If deformation of the droplet reaches to the breakup condition of Eq. (6), the breakup happens. The new radius of droplet is given by

$$\frac{r_{old}}{r_{new}} = \frac{1}{C_1}\left(\frac{7}{3} + \frac{\rho_1 r_{old}^3}{8\sigma}\ddot{y}^2\right) \qquad (7)$$

where, C_1 is the breakup constant, which is determined based on the comparison with the experimental SMD distribution. To consider the effect of drop deformation on the drag coefficient, the drag calculation process is changed as suggested by Hwang et al. (1996)

$$C_D = C_{D,sphere}(1 + 2.632y) \qquad (8)$$

where, the drag coefficient, y in Eq. (8) was calculated using

$$y = \min\left(1, \left\{\frac{a}{r} - 1\right\}\right) \qquad (9)$$

4. Results and Discussion

4.1 Determination of breakup constant C_1

To determine the breakup constant C_1 of Eq. (7), the calculated SMD distributions for various C_1 were compared with the measured results. It can be inferred from Eq. (7) that the calculated SMD is increased with the increment of C_1. The optimum value of C_1 can be found by varying C_1 from 0.6 to 1.0. In the case of 0.8, a reasonable agreement between calculated and measured result was obtained as illustrated in Fig. 4. Referring to this, the value of C_1 is set equal to 0.8 in this study.
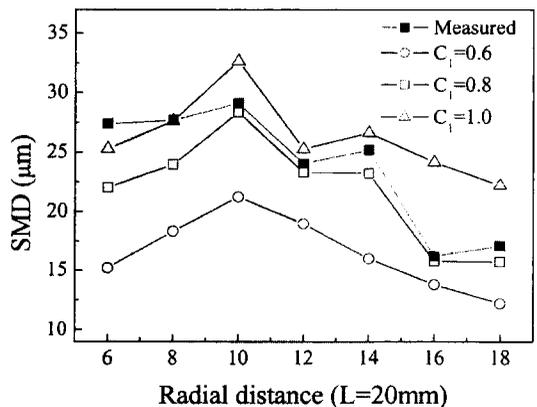

Fig. 4 Determination of the breakup constant, C_1

4.2 Development of global spray

Spray development process obtained from visualization system and KIVA-3 code with LISA-DDB hybrid model at the injection pressures of the 5 MPa and 7 MPa is illustrated in Fig. 5. The images from calculation show a reasonable accordance with the spray image of experiment. After injection, the droplets located at the down region of the spray dispersed more rapidly with the increase of injection pressure. Because the dispersed droplets have little momentum, they go upward due to the circulation of the surrounding gas. From this reason, the upward ring shaped vortex is made. In the case of 7 MPa of injection pressure the vortex is lager than that of 5 MPa, that is, the increase of injection pressure has effect on the creation of vortex on the spray outer surface. It is probable that the high injection pressure induces the high gas flow velocity, which promotes the atomization of the spray. This phenomenon makes the small droplet go upward with the guidance of surrounding gas flow. It is observed that the predicted upward vortex ring in Fig. 5 is larger than the that of experimental images. It is conjecturable that the surrounding gas flow calculated from KIVA code is somewhat
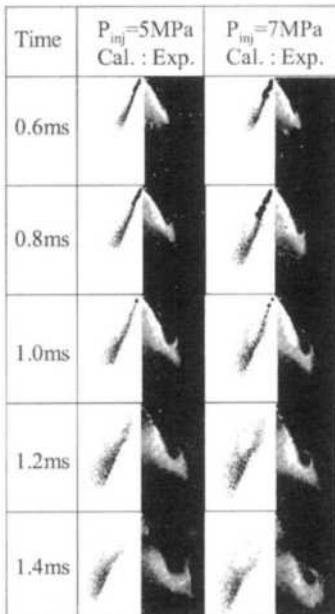
different from the actual one. In this calculation RNG $k-\varepsilon$ model is used for turbulence calculation. The calculated process of spray development with gas entrainment according to the time after injection is illustrated in Fig. 6. After injection the velocity of gas increased due to droplets with high velocity and droplets cause the gas flow to circulate through the spray as shown in Fig. 6(a), (b). While droplets moves downstream from the injector tip, the droplets split into small ones. The gas vortex tends to carry the small droplets upwards, and finally the vortex cloud is made as illustrated in Fig. 6(c), (d).
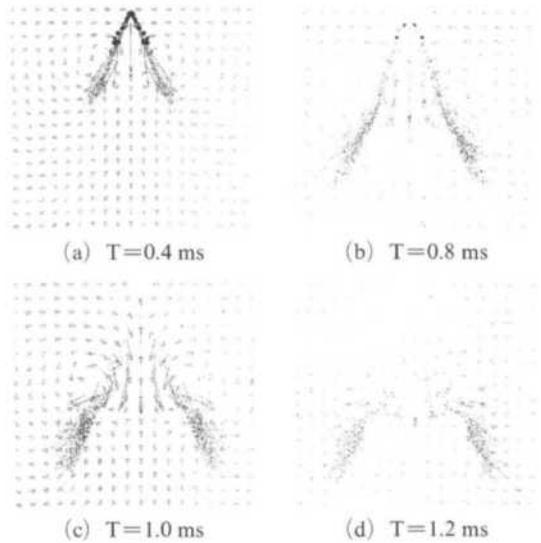

(a) T=0.4 ms   (b) T=0.8 ms

(c) T=1.0 ms   (d) T=1.2 ms

Fig. 6   Spray induced gas entrainment
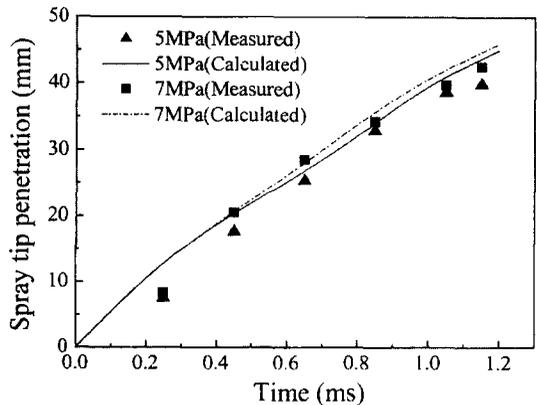

Fig. 5   Spray development process

Fig. 7   Effect of injection pressure on the spray tip penetration

Figure 7 shows measured and calculated spray tip penetrations versus time after injection at different injection pressures. In this work, the spray tip penetration is defined as the maximum distance at which the spray reaches when it is injected into stagnant air. The measured and calculated results show similar tendency, but the measured penetration is shorter than the predicted at the early stage of injection. It is probable that the predicted drag near the injector is smaller than the actual value.

5. Atomization Characteristics

To research the atomization characteristics of hollow-cone gasoline injector, the SMD distributions according the radial distance and the injec-

tion pressure are investigated experimentally and numerically as shown in Fig. 8. The droplet SMD is increased with the increase of radial distance from axis of nozzle to the passage of main spray, and SMD is decreased after that region. But this phenomenon disappears in the case of 7 MPa of injection pressure and 40 mm of axial distance from nozzle tip. It is probable that the breakup process has almost ended in that region, so the distribution of SMD is plane. Figure 9 shows the effect of injection pressure on the axial mean velocity distribution at 20 mm of the axial distance from the nozzle tip. On the whole, the predicted values are smaller than the experimental results because of the improper prediction of drag and breakup. Considering that drag calculation near the injector is underestimated and the predicted SMD shows a reasonable agreement with the measured value in Figs. 8 and 9, it can be concluded that the drag is overestimated generally but underestimated near the injector. It is probable that the LISA model does not generate atomization until the breakup length, so that the large droplets exist near the injector.

Figure 10 shows the effect of injection pressure on the calculated overall SMD as a function of time after start of injection. As can be seen in the figure, the overall SMD is decreased with the increase of injection pressure. It can be guessed that the large relative velocity between the droplet and ambient gas causes the high drag, and pro-
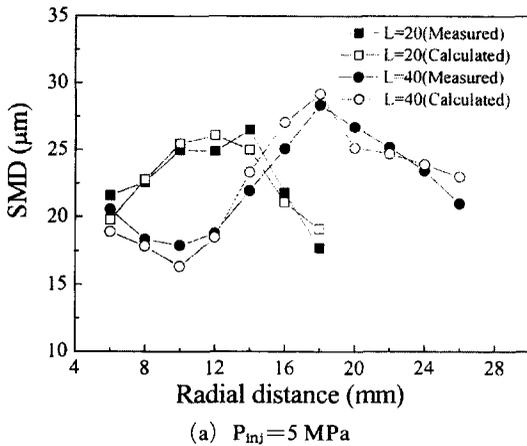
(a) P_{inj}=5 MPa
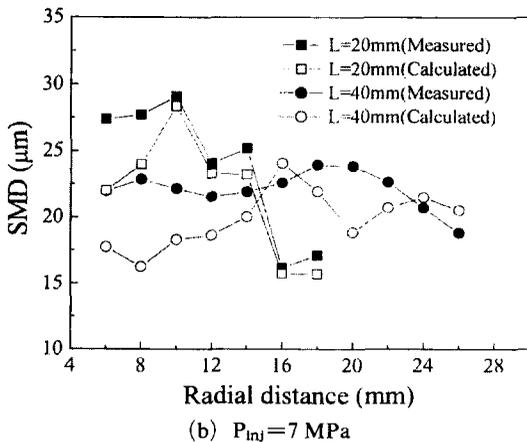
(b) P_{inj}=7 MPa

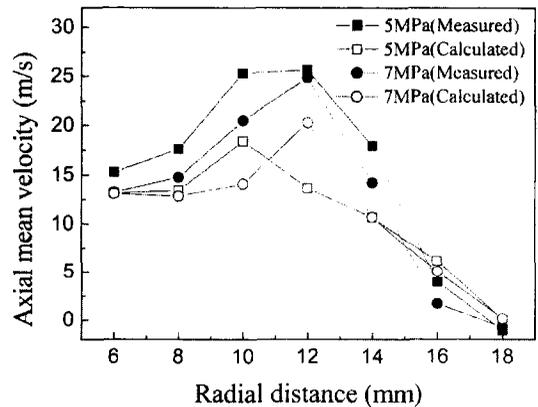**Fig. 8** Patterns of SMD distribution according to injection pressure

Fig. 9 Effect of injection pressure on the axial mean velocity distribution (L=20 mm)

motes the atomization of the injected fuel spray. After injection, the reduction ration of SMD is decreased rapidly, and reaches to almost zero at 1ms after injection.

Figure 11 illustrates the percentage distributions of LISA breakup and DDB breakup. This figure shows the regional distribution where the primary and secondary breakups are occurred. In this figure the percentage is obtained by dividing the count of droplet breakup in 0.5 mm × 0.5 mm area by the count of breakup in all area. The primary breakup caused by LISA model concentrated near the injector, and the secondary breakup governed by DDB model occurs after reaching
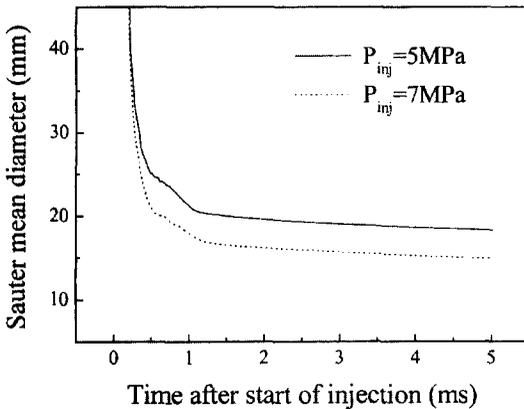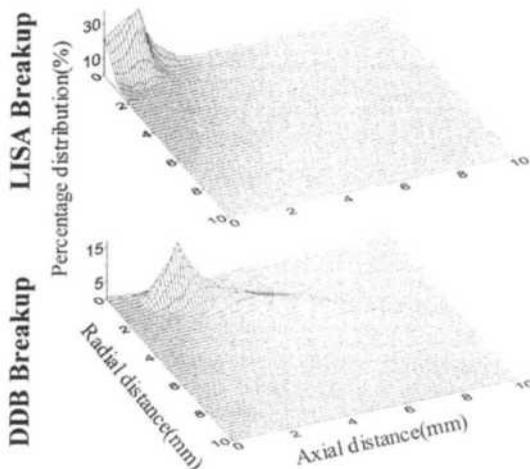
the peak value of the primary breakup.

6. Conclusions

Experimental and numerical analysis were was performed to obtain the effect of injection pressure on the development of global spray and atomization characteristics. Phase Doppler particle analysis system, visualization system with Nd : YAG laser, and LISA-DDB hybrid model are used for experiment and calculation. The conclusions of this study are summarized as follows.

(1) In this study the predicted results such as spray behaviors, droplet size, and mean velocity of the spray from LISA-DDB hybrid model show a reasonable agreement with experimental results. In this simulation, the optimum value of breakup constant, C_1, is determined to 0.8.

(2) In the case of 7 MPa of injection pressure the vortex is larger than that of 5 MPa, that is, the increase of injection pressure has effect on the creation of vortex on the spray outer surface. It can be guessed that the high injection pressure induces the high gas flow velocity, which promotes the atomization of the spray. This phenomenon makes the small droplet go upward with the guidance of surrounding gas flow.

(3) In the case of the numerical and experimental results, the mean droplet size (SMD) is increased with the increase of radial distance from axis of nozzle to the passage of main spray, and droplet SMD is decreased after that region at the 5 MPa and 7 MPa. The drag calculation is overestimated generally but underestimated near the injector. It is probable that the LISA model does not generate atomization until the breakup length, therefore the large droplets exist near the injector.

(4) The primary breakup is concentrated near the injector, and the secondary breakup occurs after reaching the peak value of the primary breakup.

Fig. 10 Overall Sauter mean diameter as a function of time

Fig. 11 Percentage distributions of primary and secondary breakups

Acknowledgment

References

Dombrowski, N. and Johns, W. R., 1963, "The Aerodynamic Instability and Disintegration of Viscous Liquid Sheets," *Chem. Eng. Sci.*, Vol. 18, pp. 203~214.

Hwang, S. S., Liu, Z. and Reitz, R. D., 1996, "Breakup Mechanisms and Drag Coefficients of High-Speed Vaporizing Liquid Drops," *Atomization and Sprays*, Vol. 6, pp. 353~376.

Ibrahim, E. A., Yang, H. Q. and Przekwas, A. J., 1993, "Modeling of Spray Droplets Deformation and Breakup," *AIAA J. Propulsion and Power*, Vol. 9, No. 4, pp. 652~654.

Kim, J. I., No, S. Y., Kim, J. O. and Lim, J. H., 1999, "Modeling Capability of Various Atomization and Droplet Breakup Models for DI Diesel Engines," *The Eighth Symposium (ILASS-Japan) on Atomization*, Osaka, Japan, pp. 149~154.

Lee, C. S., Chon, M. S. and Park, Y. C., 2001, "Spray Structure of High-Pressure Gasoline Injectors in a Gasoline Direct-Injection Engine," *International Journal of Automotive Technology*, Vol. 2, No. 4, pp. 165~170.

Li, S. C. and Gebert, K., 1998, "Spray Characterization of High Pressure Gasoline Injectors with Swirl and Non-Swirl Nozzles," *SAE paper*, 981935.

O'Rourke, P. J. and Amsden, A. A., 1987, "The tab Method for Numerical Calculation of Spray Droplet Breakup," *SAE paper*, 872089.

Park, S. W., Kim, H. J. and Lee, C. S., 2003, "Numerical and Experimental Analysis of Spray Atomization Characteristics of a GDI Injector," *KSME International Journal*, Vol. 17, No. 3, pp. 449~456.

Reitz, R. D., 1987, "Modeling Atomization Processes in High-Pressure Vaporizing Sprays," *Atomisation and Spray Technology*, Vol. 3, pp. 309~357.

Schmidt, D. P., Nouar, I., Senecal, P. K., Rutland, J. K. and Reitz, R. D., 1999, "Pressure-Swirl Atomization in the Near Field," *SAE paper*, 1999-01-0496.

Senecal, P. K., Schmidt, D. P., Nouar, I., Rutland, J. K. and Reitz, R. D., 1999, "Modeling High-Speed Viscous Liquid Sheet Atomization," *International Journal of Multiphase Flow*, Vol. 25, pp. 1073~1097.